RSC Advances

ROYAL SOCIETY OF CHEMISTRY

www.rsc.org/advances

Advanced treatment of acrylic fiber manufacturing wastewater with a combined microbubble-ozonation/ultraviolet irradiation process

Tianlong Zheng,[a] Tao Zhang,[b] Qunhui Wang,[a,c*,] Yanli Tian,[a] Zhining Shi,[d] Nicholas Smale,[e] and Banghua Xu,[a]

Abstract

This work investigated the effectiveness of a combination of microbubble-ozonation and ultraviolet (UV) irradiation for the treatment of secondary wastewater effluent of a wet-spun acrylic fiber manufacturing plant. Under reactor condition (ozone dosage of 48 mg/L, UV fluence rate of 90 mW/cm^2, initial pH of 8.0, and reaction time of 120 min), the biodegradability (represented as BOD_5/COD_{cr}) of the wastewater improved from 0.18 to 0.47. This improvement in biodegradability is related to the degradation of alkanes, aromatic compounds, and other bio-refractory organic compounds. The combination of microbubble-ozonation and UV irradiation synergistically improved treatment efficiencies by 228%, 29%, and 142% for COD_{cr}, UV_{254} removal and BOD_5/COD_{cr} respectively after 120 min reaction time, as compared with the sum efficiency of microbubble-ozonation alone and UV irradiation alone. Hydroxyl radical production in the microbubble-ozonation/UV process was about 1.8 times higher than the sum production in microbubble-ozonation alone and UV irradiation alone. The ozone decomposition rate in the combined process was about 4.1 times higher than that in microbubble-ozonation alone. The microbubble-ozonation/UV process could be a promising technique for the treatment of bio-refractory organics in the acrylic fiber manufacturing industry.

Keywords: combined advanced oxidation process; hydroxyl radical; microbubble-ozonation/UV; synergistic effects; wet-spun acrylic fiber manufacturing wastewater.

a. Department of Environmental Engineering, University of Science and Technology Beijing, 30 Xueyuan Road, Haidian District, Beijing 100083, China;
b. Water Desalination and Reuse Center, King Abdullah University of Science and Technology, Thuwal 4700, Saudi Arabia;
c. Beijing Key Laboratory of Resource-oriented Treatment of Industrial Pollutants, University of Science and Technology Beijing, 30 Xueyuan Road, Haidian District, Beijing 100083, China;
d. School of Earth and Environmental Sciences, The University of Adelaide, South Australia 5005, Australia;
e. The Bionics Institute, Victoria, Australia 3002, Australia.
†* Corresponding author: Qunhui Wang; E-mail: wangqh59@sina.com; Tel: +86 -010- 62332778; Fax:: +86- 010- 62332778

1. Introduction

Wastewater produced in wet-spun acrylic fiber manufacturing industry contains numerous bio-refractory organic pollutants such as organic nitriles, alkanes, aromatic compounds, esters, phenols, and amides.[1] If not properly handled, such wastewater can severely pollute receiving waters. There is still no fully mature biological treatment technique for the comprehensive treatment of wet-spun acrylic fiber manufacturing wastewater to meet effluent discharge standards.

The microbubble-ozonation technique has been widely used in the treatment of bio-refractory industrial wastewater.[1-3] This technique has overcome some of the limiting factors of the traditional ozonation process such as low ozone dissolution and slow gas-liquid mass transfer rate.[4] The generation of hydroxyl free radicals (•OH) from ozone can improve the oxidation effects as •OH possesses a higher oxidation potential than molecular ozone.[5] Hydroxyl radical generation can be improved during microbubble ozone intrusion.[6] More recently, has been found that microbubble collapse in microbubble-ozonation also promotes hydroxyl radical production.[7, 8] However, the generation rate of hydroxyl radicals in the microbubble-ozonation process is still not high enough for efficient degradation of refractory organic pollutants especially when the concentration of these pollutants is relatively high. Ultraviolet (UV) irradiation enhances •OH production during ozonation treatment because of the photolysis of ozone.[9-12] Microbubble and UV irradiation enhanced ozonation has not yet been investigated in the literature, and couple be a promising technology for advanced treatment of bio-refractory wastewater, especially for the wet-spun acrylic fiber manufacturing wastewater (having high concentrations refractory organic pollutants).

In this study, the microbubble-ozonation/UV combined process was applied to treat the secondary effluent of a wet-spun acrylic fiber manufacturing plant. We optimized reactor parameters (i.e., ozone dosage, UV fluence rate, initial pH and reaction time), and then, investigated removal rates of the contaminants and improvement of biodegradability under the optimized treatment condition. This new combined process was assessed by an experimentally determined synergistic effect, quantification of hydroxyl radical production, and ozone decomposition rate.

2. Experimental

2.1. Wastewater

The experimental wastewater was secondary effluent of an acrylic fiber manufacturing wastewater in Northern China. The wastewater was stored at 4 °C before use. Physical and chemical properties of the wastewater are shown in Table 1. This wastewater is characteristic in its complex organic components, high toxicity, and low biodegradability.

Table1. Characteristics of the acrylic fiber wastewater from all 90 experimental batches.

2.2. Experimental setup

The experimental apparatus is shown in Fig. 1. The reactor was made of transparent rigid Plexiglas with an inner

diameter of 80 mm, a height of 1200 mm, and an effective volume of 6 L. A TCRI Microbubble Generator (Japan) was used to produce microbubbles, with a mean bubble diameter of less than 45 μm under the operational pressure of 0.4 MPa. For comparative purposes, a cylindrical 40 μm micropore titanium plate placed at the bottom of the reactor was used to generate ozone macrobubbles (with a mean bubble diameter of approximately 1 mm) with ozone gas produced by an ozone generator (CF-YG5, Shanmei Shuimei Co. Beijing) at a rate of 5 g O_3/hr, using dehumidified air as gas source (flow rate of air of 0.5L/min). In addition, a low-pressure mercury vapor UV lamp equipped within a quartz well was submerged through the centre of the reactor. Five UV lamps (i.e., 10 W (15 mm diameter × 212 mm height), 14 W (15 mm diameter × 303 mm height), 18 W (15 mm diameter × 356 mm height), 23 W (15 mm diameter × 436 mm height), and 28 W (15 mm diameter × 550 mm height) produced by Cnlight Co., Ltd, Guangdong, China) were used to investigate the influence of irradiation intensity. The UV fluence rate[13] of the above described UV lamps at distance of 4 cm from the centre were 50, 70, 90, 114 and 139 mW/cm^2, respectively.

Fig. 1. Schematic diagram of microbubble-ozonation/UV combined process experimental setup.

At the beginning of the experiment, 3 L of secondary acrylic fiber manufacturing wastewater was pumped into the reactor with a peristaltic pump. When the microbubble-ozonation/UV combined process was activated, the macrobubble pathway was closed, and vice versa. In the microbubble-ozonation/UV process, the wastewater was continuously circulated between the microbubble generator and the reactor.

Ozone gas exhausted from the reactor was absorbed with 2% KI solution. The temperature of the reaction solution maintained at 20 °C throughout the experiment. Samples withdrawn at predetermined time intervals were immediately purged with nitrogen gas to remove residual ozone. For gas chromatography-mass spectrometry (GC-MS) analysis, the residual ozone was not purged, but rather was left to decompose over two days.

2.3. Analysis

Most of the wastewater quality parameters were measured according to *The Water and Wastewater Monitoring and Analysis Method (4th Edition)*.[14] In addition, COD_{cr}, BOD_5, TOC, and UV_{254} were respectively measured by a COD rapid digestion apparatus (DIS-1A, Shenzhen Changhong Instrument, Co., Ltd, China), oxiTop system (OxiTop, WTW, Germany), vario TOC analyzer (vario TOC, Elementar, Germany) and an UV-visible spectrophotometer (UV-752, METASH, China). The toxicity of samples was analyzed using Modulus Single Tube Luminometer (Turner Biosystems, USA), which is based on the light emission inhibition of luminescent bacteria, the methods of which can be found in Martins et al.[15] Further, the toxicity level expressed as EC_{50}, representing samples concentrations causing 50% bacteria inhibition, was acquired using the dilution of each sample. The dissolved oxygen concentration and the pH were determined with a dissolved oxygen meter (HQ30D, Hach, USA) and an automatic potentiometric titrator meter (ZD-2, LEICI, China) respectively at 20 °C. The pH for all solution used in this experiment was adjusted by adding 0.1 mol/L of HCl or NaOH solution, controlling it at the desired level. The gaseous

ozone concentration was measured with the iodometric method.[16] The concentration of dissolved ozone was tested with the indigo colorimetric method (Standard Method 4500-O_3 B).[17]

The hydroxyl radical concentration was determined with a three-dimensional excitation-emission matrix fluorescence spectroscopy (3D-EEM) (F2700, Hitachi, Japan) after reaction with disodium salt of terephthalic acid (NaTA) and filtration with a 0.45 μm PVDF membrane. NaTA reacts with hydroxyl radicals to form 2-hydroxyterephthalic acid (HTA) that gives a bright stable fluorescence ($\lambda_{emission}$ = 425 nm, $\lambda_{excitation}$ = 315 nm).[18] TA and NaTA are extensively applied to detect hydroxyl radicals produced in aqueous phase.[19, 20] In this study, samples (5 mL) collected from the reactor were reacted with 0.5 mM NaTA (5 mL) at the pH of 6.85 in which the buffer was 10 mM mixed non-fluorescent phosphate solution. The samples were analyzed within a few hours of being collected. EEM spectra were scanned from 200 to 450 nm for excitation and 280 to 500 nm for emission.

GC-MS was used for the analysis of the main organic compounds in the wastewater. The wastewater sample (150 mL) was extracted with 50 mL of CH_2Cl_2 (Chromatogram Pure Grade, Fisher, USA) under acidic (pH 2.0), neutral (pH 7.0), and alkaline (pH 12.0) conditions. The three extracts were mixed together, dehydrated with anhydrous sodium sulfate and dried under the flow of nitrogen gas. The residual was dissolved in 1.0 mL of CH_2Cl_2 and then 1 μL of the solution was injected into a Shimadzu GCMS-QP2010 plus system (Shimadzu., Japan) and separated with a capillary column (30 m × 0.25 mm i.d., J&W Scientific 122-5032 DB-5 , USA) . The GC oven temperature was maintained at 50 °C for 1 min, raised at a rate of 10 °C min^{-1} to 60 °C (held for 2 min), and then further raised at 10 °C min^{-1} to 250 °C (held for 5 min). Injector port, interface and ion source temperatures were 250, 280 and 300 °C, respectively. MS was operated in electron ionization mode (EI) at 70 eV. Identification of the compounds was based on the NIST 05 mass spectral library database.

COD_{cr} etc means were calculated from three independent runs of the reactor, with values given as mean ± standard deviation throughout the text.

3. Results and Discussion

3.1. Optimization of process parameters

Treatment was carried out under different conditions of ozone dosage, UV fluence rate and pH to achieve the maximum COD_{cr} removal rate (shown in Fig. 2.).

Fig. 2. Influences of different parameters on the COD_{cr} removal efficiency in the microbubble-ozonation/UV combined system. (a) ozone dosage, (b) UV fluence rate, (c) initial pH and (d) reaction time. Error bars represent standard deviation of three runs.

In order to determine the effect of the ozone dosage on COD_{cr} removal, ozone concentrations were tested at 6, 12, 24, 36, 48, 60 and 72 mg/L with UV fluence rate, initial pH and reaction time being fixed at 50 mW/cm^2, 8.0 and 120 min respectively. Fig. 2a shows that the COD_{cr} removal increased from 9.5% to 56.7% as the ozone dosage was increased from 6

to 48 mg/L. Much less improvement in COD_{cr} removal (3.4%) was observed when the ozone dosage was further increased to 72 mg/L.

The influence of UV fluence rate on the COD_{cr} removal was investigated at 50, 70, 90, 114 and 139 mW/cm^2 with ozone dosage of 48 mg/L, initial pH of 8.0 and a reaction time of 120 min. Fig. 2b shows that the COD_{cr} removal increased from 58.7% to 85.4% as the UV fluence rate was increased from 50 to 90 mW/cm^2. The COD_{cr} removal rate increased slightly when the UV fluence rate was increased continuously. Because of the limited benefit at the higher UV fluence rate, the UV fluence rate of 90 mW/cm^2 was selected for further optimization.

According to the literature,[11, 12] pH is a crucial parameter that influences contaminant removal during O_3/UV treatment. Since the type of oxidant generated greatly depends on reaction pH,[21] the effect of the initial pH on COD_{cr} removal in the microbubble-ozonation/UV system was tested in the range of 3 to 11, while ozone dosage, UV fluence rate and reaction time were kept at 48 mg/L, 90 mW/cm^2 and 120 min, respectively. Fig. 2c shows that the COD_{cr} removal rate reached its highest (87.3%) at the pH of 8.0, and then decreased as pH was further increased. There are two well-established oxidation pathways for ozone: ozone direct oxidation and indirect oxidation by hydroxyl radicals generated from ozone decomposition.[22, 23] Direct oxidation, the predominate form of ozone oxidation in acidic media, has a greater selectivity for organics than hydroxyl radical oxidation.[24] In contrast, the indirect oxidation by non-selective hydroxyl radicals is the main oxidation pathway of ozonation under alkaline conditions.[25] At neutral pH, both oxidation pathways contribute to the degradation of bio-refractory matter.[26] Therefore, the above described relatively lower COD_{cr} removal at acidic to neutral pH than that at pH of 8.0 can be attributed to the relatively weaker oxidation ability of ozone molecules than hydroxyl radicals which was generated from ozone-OH^- reaction. Besides, at the acidic to neutral pH, free radicals are not formed, which results in few free hydroxyl radicals forming. In general, the generation rate of hydroxyl radicals in an alkaline medium (pH>8.0) can be greater than that at pH of 8.0,[27] thus, higher contaminants degradation should be achieved. However, since copolymers (such as acrylate and acrylamide) formed under an alkaline medium during hydroxyl radical oxidation, the wastewater will be much more difficult to remove than the parent compound,[28] which could be the reason for the decline of COD_{cr} removal when the pH was further increased. The optimal pH value was determined to be 8.0.

The effect of the reaction time on the COD_{cr} removal rate was investigated at ozone dosage of 48 mg/L, UV fluence rate of 90 mW/cm^2 and an initial pH of 8.0. Fig. 2d shows that the COD_{cr} removal rate gradually increased to 87.5% at 120 min. Further, prolonging the reaction for a further 1 h caused only a 4.2% increase in COD_{cr} removal. In consideration of the economic cost of an increased reaction time, we consider the optimal reaction time of this process to be 120 min.

3.2. Biodegradability improvement under optimal condition

The removal of contaminants in terms of COD_{cr}, BOD_5, TOC, UV_{254}, and BOD_5/COD_{cr} ratio were investigated under the above optimized reaction conditions (i.e., ozone dosage of 48 mg/L, UV fluence rate of 90 mW/cm^2, initial pH value of 8.0 and reaction time of 120 min) (Fig. 3).

Fig. 3. Degradation of contaminants over time in the microbubble-ozonation/UV reactor under optimized conditions (i.e., ozone dosage of 48 mg/L, UV fluence rate of 90 mW/cm^2, initial pH value of 8.0 and reaction time of 120 min). Error bars represent standard deviation of three runs.

Fig. 3 shows that the COD_{cr} decreased by 87.6% (from 322 ± 25 to 39.8 ± 3.6 mg/L), and UV_{254} by 87.7% (from 0.42 ± 0.05 to 0.05 ± 0.004 Abs/cm^{-1}), over the course of the reaction. BOD_5 decreased from 59 ± 16 to 23.5 ± 7.1 mg/L in 30 min, and then slightly increased and maintained a stable level for the remaining reaction. TOC decreased from 113 ± 19 to 31.8 ± 7.4 mg/L, indicating that approximately 63.0% of TOC was eliminated in the combined treatment process. Further, the calculated BOD_5/COD_{cr} ratio decreased from 0.18 ± 0.02 to 0.10 ± 0.02 in the first 30 min, and then increased to 0.47 ± 0.03 after 120 min, demonstrating an increased biodegradability. The variation in BOD_5/COD_{cr} is similar to that found by Martins et al.[15] through the Fenton exudation process applied to phenolic wastewater. This above described result can be supported by the variation of toxicity in wastewater, where the toxicity of treated wastewater was only 13.6% of that of raw wastewater (EC_{50} of raw sample was 17.5%). In addition, the improved biodegradability of the wastewater could also be explained by the removal of bio-refractory organic compounds in the microbubble-ozonation/UV combined process. Therefore, the changes of contaminants in raw and treated wastewater were verified by GC-MS analysis. Organic compounds identified in the raw wastewater through GC-MS (Fig. 4a) are summarized in Table 2.

These compounds include 11 alkanes (accounting for 68.6% total peak area), 5 aromatic compounds (accounting for 25.3% total peak area), and 3 esters (accounting for 2.8% total peak area). A small number of phenols (2, 2.5%), an organic nitrile (1, 0.4%), and an amide (1, 0.3%) were also identified. Among these long-chain alkane compounds, the carbon numbers of alkanes (except decane) varied from 15 to 40, which are bio-refractory for natural water bodies.[29] Both aromatic compounds and organic nitriles are toxic and are difficult to eliminate through natural biodegradation.[30] Therefore, the poor biodegradability of the raw wastewater probably is due to the presence of these bio-refractory organic compounds.

Fig. 4. GC-MS chromatographs of (a) raw wastewater and (b) treated by combined microbubble-ozonation/UV process.

Table 2. The main organic pollutants identified in the secondary effluent with GC-MS.

By comparison to Fig 4a, the chromatograph of Fig. 4b shows that most organic pollutants were significantly removed after the microbubble-ozonation/UV treatment. The compounds remaining in the effluent were long-chain alkanes, nevertheless, more than 87.0% of alkane peak area was eliminated. Based on overall performance, it can be concluded that organic compounds with high molecular weight were converted into smaller molecules with easier biodegradable characteristics, which is supported by the improved biodegradability and decreased toxicity of the effluent. This result is similar to that derived by Gong et al. [31] who reported the organic contaminants in treated samples was easy to degrade with

the analysis of BOD_5 and toxicity. Therefore, the microbubble-ozonation/UV combined process is an effective technique for the treatment of secondary wet-spun acrylic fiber manufacturing wastewater.

3.3. Synergistic effect

3.3.1. Synergistic effect of microbubble-ozonation and UV in contaminant removal

The removal rates of COD_{cr} and UV_{254} in microbubble-ozonation/UV combined process and separated processes (i.e., microbubble-ozonation alone and UV irradiation alone) are shown in Fig. 5.

Fig. 5. The removal efficiency of COD_{cr} and UV_{254} in microbubble-ozonation/UV combined process and separated processes. Error bars represent standard deviation of three runs.

Fig. 5 shows that UV irradiation alone only reduced 5.0% COD_{cr} of the wastewater in 120 min; the COD_{cr} slightly increased in the first 60 min. The UV_{254} removal rate of UV irradiation alone was 14.1% in 120 min. The microbubble-ozonation achieved better removal rates for COD_{cr} and UV_{254} (i.e., 23.2% and 50.5%, respectively), which could be ascribed to greater amounts of hydroxyl radicals being generated during the collapse of ozone microbubbles as well as the self-decomposition of ozone in water at the pH of 8.[1, 2, 32, 33] The microbubble-ozonation/UV combined process removed COD_{cr} by 92.5% and UV_{254} by 83.4%, which is much higher than the sum of individual removal rates of the two separated processes.

The synergistic efficiency of microbubble-ozonation UV process is defined as:

$$\eta = \frac{R_{O_3/UV} - (R_{O_3} + R_{UV})}{R_{O_3} + R_{UV}} \times 100\% \qquad \text{(A)}$$

where R_{O_3}, R_{UV}, and $R_{O_3/UV}$ represent the removal rate or improvement extent of biodegradability in microbubble-ozonation alone, UV alone, and the combined microbubble-ozonation/UV process, respectively. As calculated with Eq. (A), the synergistic efficiencies in COD_{cr} and UV_{254} removal and BOD_5/COD_{cr} improvement in 120 min are shown in Table 3.

Table 3. Variation of COD_{cr}, UV_{254}, and BOD_5/COD_{cr} in microbubble-ozonation alone, UV alone, and the combined microbubble-ozonation/UV process after 120 min reaction.

Table 3 indicates that the microbubble-ozonation/UV combined process has a good performance with the synergistic efficiencies in COD_{cr} and UV_{254} removal and BOD_5/COD_{cr} improvement in 120 min reaction being 228%, 29%, and 142%, respectively. Based on a great number of hydroxyl radicals in microbubble-ozonation, the introduced UV irradiation technology can also effectively enhance the production of hydroxyl radicals from ozone.[34] Therefore, the significant improvement in contaminant degradation in the combined process is achieved. In addition, the activation energy of the reaction could also be reduced by UV irradiation, contributing to organic contaminant degradation.

3.3.2. The generation of hydroxyl radicals

In general, hydroxyl radicals reacts very quickly with organics with reaction rate constants being 10^6 to 10^{10} $M^{-1}s^{-1}$, while molecular ozone is much less reactive (reaction rate constants of 10^{-5} to 10^{-1} $M^{-1}s^{-1}$).[35-38] The high degradation rates of refractory organic pollutants of the wastewater in the microbubble-ozonation/UV combined process possibly were mainly due to hydroxyl radical oxidation. In order to verify the main pathway of COD_{cr} elimination by hydroxyl radicals or ozone molecules, *tert*-butyl alcohol (*t*-BuOH) used as a radical scavenger since it reacts briskly with free hydroxyl radicals ($k_{\bullet OH,t\text{-}BuOH}$ = 5×10^8 $M^{-1}s^{-1}$), but very slowly with ozone, $k_{O3,t\text{-}BuOH}$ = 3×10^{-2} $M^{-1}s^{-1}$.[39] The experiment was conducted under previously stated optimal conditions at different concentration of *t*-BuOH (Fig. 6).

Fig. 6. The influence of *t*-BuOH concentration on COD_{cr} removal for the combined microbubble-ozonation/UV process; Error bars represent standard deviation of three runs.

Fig. 6 shows that the COD_{cr} removal was significantly inhibited by the increase of *t*-BuOH concentration (The contribution of *t*-BuOH to COD_{cr} was totally eliminated with the result of a control test). The previous COD_{cr} removal rate of 92.5% rapidly decreased to 40.1% at *t*-BuOH concentrations of 0 and 50 mg/L, respectively. When the concentration of *t*-BuOH was increased continuously, the COD_{cr} removal inhibited slightly, which could be considered as all of the hydroxyl radicals produced in microbubble-ozonation/UV process was scavenged by *t*-BuOH of 50 mg/L. The hydroxyl radical would have contributed approximately 56.6% of the COD_{cr} removal.

Fig. 7. The quantities of hydroxyl radicals produced in ozone water, UV water and the combined ozone/UV water under different conditions as represented with 3D-EEM intensity of the HTA generated.

The relative amount of hydroxyl radicals produced in the ozone water, UV water and the combined ozone/UV water under different conditions was compared with the fluorescence intensity of HTA (produced from hydroxyl radical-NaTA reaction) recorded with 3D-EEM (Fig. 7). The quantities of hydroxyl radicals of the samples from microbubble-ozonation process alone was much higher than that from the macrobubble-ozonation process and UV irradiation alone, which lead to a better achievement (described above) for the microbubble-ozonation process alone. A similar result was derived by Chu et al.[2] who reported that the fluorescence intensity of the samples from the microbubble system was much higher than that from the bubble contactor.. In addition, there was almost no fluorescence detected in the presence of the hydroxyl radical scavenger *t*-BuOH of 50 mg/L in the ozone water sample, which also supported the results of the inhibitation concentration of *t*-BuOH for hydroxyl radical during microbubble-ozonation/UV process. Interestingly, the quantities of hydroxyl radicals in the microbubble-ozonation/UV combined process during the treatment of the wastewater were significantly higher than the summation of these in microbubble-ozonation alone and UV alone: the peak area of the former was 1.8 times higher than the summation of the latter two processes. This result clearly shows that UV irradiation and microbubble-ozonation have a

synergetic effect in the degradation of the contaminants in the wastewater.

3.3.3. The acceleration of ozone decomposition

Dissolved ozone is unstable in aqueous solution, and readily decomposes to free radicals, particularly hydroxyl radicals. UV, metal oxides, and certain other catalysts can enhance the ozone decomposition rate. The ozone decomposition rates of the microbubble-ozonation/UV combined process, microbubble-ozonation alone, and macrobubble-ozonation alone were tested. The reactor containing 4 L of deionized water were bubbled with ozone gas for 10 min at an inlet gas flow of 0.5 L min^{-1} and an ozone dosage of 48 mg/L. Then, samples were collected at predetermined time intervals after the bubbling. For the microbubble-ozonation/UV combined process, the reactor was irradiated by UV light (90 mW/cm^2) after the bubbling.

Fig. 8. The influence of UV irradiation and aeration approaches on ozone decomposition.

The ozone decomposition rates of the microbubble-ozonation/UV combined process, microbubble-ozonation alone, and macrobubble-ozonation alone can be well fitted with first-order reaction kinetics (Fig. 8) with rate constant (k_d) being 0.5233 min^{-1}, 0.1264 min^{-1} and 0.0651 min^{-1}, respectively. The k_d of microbubble-ozonation alone was 1.9 times higher than that in the macrobubble-ozonation alone, indicating that the use of microbubbles can effectively improve the ozone decomposition rate. This conclusion is consistent with Liu et al.[3] who found that the dissolved oxygen concentration in ozone-microbubble system was much higher than that in air-microbubble system, which was ascribed to the higher transformation from ozone to oxygen of the former at higher ozone decomposition rate. The k_d of microbubble-ozonation/UV combined process was 4.1 times higher than that of the microbubble-ozonation alone. Chang et al.[40] also found that UV-C radiation in the ozonation process can promote the decomposition of O_3 to form •OH radical. Therefore, the much higher ozone decomposition rate in the combined process can explain why more hydroxyl radicals were generated in this process, which can further decompose the organic contaminates in wastewater.

4. Conclusion

For the selected secondary wet-spun acrylic fiber manufacturing wastewater, 87.6% of COD_{cr}, 68.0% of BOD_5, 71.9% of TOC, and 87.7% of UV_{254} can be removed by the microbubble-ozonation/UV combined process under optimal conditions (ozone dosage of 48 mg/L, UV fluence rate of 90 mW/cm^2, initial pH value of 8.0, and reaction time of 120 min). Biodegradability (BOD_5/COD_{cr}) was also improved from 0.18 to 0.47, which was ascribed to the degradation of refractory contaminants such as alkanes and aromatic compounds. A significant synergetic effect existed between UV irradiation and microbubble ozonation for the removal of COD_{cr} and UV_{254}, and the improvement of BOD_5/COD_{cr}, which can be attributed to an acceleration in ozone decomposition and an enhancement of hydroxyl radical generation.

Acknowledgment

The authors gratefully acknowledge the financial support of the Major Science and Technology Program for Water Pollution Control and Treatment (2012ZX07201002-6). Thanks also give to Kikuchi ECO-Earth Co. Ltd. (Tokyo, Japan) for providing the microbubble generator and China Oil HBP Science & Technology Co., Ltd for providing the wastewater.

References:

1 T. Zheng, Q. Wang, T. Zhang, Z. Shi, Y. Tian, S. Shi, N. Smale and J. Wang, *J Hazard Mater*, 2015, **287**, 412-420.

2 L. B. Chu, X. H. Xing, A. F. Yu, Y. N. Zhou, X. L. Sun and B. Jurcik, *Chemosphere*, 2007, **68**, 1854-1860.

3 S. Liu, Q. H. Wang, T. C. Sun, C. Wu and Y. Shi, *J Chem Technol Biot*, 2012, **87**, 206-215.

4 L. B. Chu, S. T. Yan, X. H. Xing, A. F. Yu, X. L. Sun and B. Jurcik, *Chemosphere*, 2008, **72**, 205-212.

5 T. E. Agustina, H. M. Ang and V. K. Vareek, *J Photoch Photobio C*, 2005, **6**, 264-273.

6 A. Agarwal, W. J. Ng and Y. Liu, *Chemosphere*, 2011, **84**, 1175-1180.

7 P. Li, M. Takahashi and K. Chiba, *Chemosphere*, 2009, **75**, 1371-1375.

8 M. Takahashi, K. Chiba and P. Li, *J Phys Chem B*, 2007, **111**, 1343-1347.

9 C. Gottschalk, J. A. Libra and A. Saupe, Application of Ozone in Combined Processes. In Wiley-VCH Verlag GmbH & Co. KGaA: 2009, 267-343.

10 S. Osbeck, R. H. Bradley, C. Liu, H. Idriss and S. Ward, *Carbon*, 2011, **49**, 4322-4330.

11 M. S. Lucas, J. A. Peres and G. Li Puma, *Sep Purif Technol*, 2010, **72**, 235-241.

12 K. Wang, J. Guo, M. Yang, H. Junji and R. Deng, *J Hazard Mater*, 2009, **162**, 1243-1248.

13 J. R. Bolton, *Water Res*, 2000, **34**, 3315-3324.

14 F. S. Wei, W. Q. Qi, Z. G. Sun, Y. R. Huang and Y. W. Shen, *China Environmental Science Press, Beijing*, 2002,

15 R. C. Martins, A. F. Rossi and R. M. Quinta-Ferreira, *J Hazard Mater*, 2010, **180**, 716-721.

16 R. Gehr, M. Wagner, P. Veerasubramanian and P. Payment, *Water Res*, 2003, **37**, 4573-4586.

17 W. A. APPA, Standard methods for the examination of water and wastewater, 21st Ed. In American Public Health Association, American Water Work Association, Water Environment federation, Washington, DC.: 2005.

18 G. J. Price and E. J. Lenz, *Ultrasonics*, 1993, **31**, 451-456.

19 M. Sahni and B. R. Locke, *Ind Eng Chem Res*, 2006, **45**, 5819-5825.

20 R. W. Matthews, *Radiat Res*, 1980, **83**, 27-41.

21 S. Jagadevan, N. J. Graham and I. P. Thompson, *J Hazard Mater*, 2013, **244–245**, 394-402.

22 J. Suave, H. J. José and R. F. P. M. Moreira, *Ozone-Sci Eng*, 2014, **36**, 560-569.

23 J. Basiri Parsa and S. Hagh Negahdar, *Sep Purif Technol*, 2012, **98**, 315-320.

24 J. Lv, Y. Li and Y. Song, *Water Res*, 2013, **47**, 4993-5002.

25 H. Kusic, N. Koprivanac and A. L. Bozic, *Chem Eng J*, 2006, **123**, 127-137.

26 E. J. Rosenfeldt, K. G. Linden, S. Canonica and U. Von Gunten, *Water Res*, 2006, **40**, 3695-3704.

27 J. Hoigne and H. Bader, *Water Res*, 1976, **10**, 377-386.

28 L. B. Krentsel, Y. V. Kudryavtsev, A. I. Rebrov, A. D. Litmanovich and N. A. Platé, *Macromolecules*, 2001, **34**, 5607-5610.

29 K. Tong, Y. Zhang, G. Liu, Z. Ye and P. K. Chu, *Int Biodeter Biodegr*, 2013, **84**, 65-71.

30 F. Widdel and R. Rabus, *Curr Opin Biotech*, 2001, **12**, 259-276.

31 C. Gong, Z. Zhang, H. Li, D. Li, B. Wu, Y. Sun and Y. Cheng, *J Hazard Mater*, 2014, **274**, 465-472.

32 P. Li, M. Takahashi and K. Chiba, *Chemosphere*, 2009, **77**, 1157-1160.

33 M. Takahashi, *J Phys Chem B*, 2005, **109**, 21858-21864.

34 T. Garoma and M. D. Gurol, *Environ Sci Technol*, 2004, **38**, 5246-52.

35 U. Von Gunten and J. Hoigne, *Environ Sci Technol*, 1994, **28**, 1234-1242.

36 E. C. Wert, F. L. Rosario-Ortiz and S. A. Snyder, *Environ Sci Technol*, 2009, **43**, 4858-4863.

37 M. S. Elovitz and U. von Gunten, *Ozone-Sci Eng*, 1999, **21**, 239-260.

38 C. Gottschalk, J. A. Libra and A. Saupe, Ozone Applications. In Wiley-VCH Verlag GmbH & Co. KGaA: 2009, 27-65.

39 J. Hoigné, Chemistry of aqueous ozone and transformation of pollutants by ozonation and advanced oxidation processes. In Springer: 1998, 83-141.

40 C. Chang, C. Trinh, C. Chiu, C. Chang, S. Chiang, D. Ji, J. Tseng, C. Chang and Y. Chen, *J Taiwan Inst Chem E*, 2014, **49**, 100-104.

Figures and tables caption:

Figures caption:

Fig. 1. Schematic diagram of microbubble-ozonation/UV combined process experimental setup.

Fig. 2. Influences of different parameters on the COD_{cr} removal efficiency in the microbubble-ozonation/UV combined system. (a) ozone dosage, (b) UV fluence rate, (c) initial pH and (d) reaction time. Error bars represent standard deviation of three runs.

Fig. 3. Degradation of contaminants over time in the microbubble-ozonation/UV reactor under optimized conditions (i.e., ozone dosage of 48 mg/L, UV fluence rate of 90 mW/cm^2, initial pH value of 8.0 and reaction time of 120 min). Error bars represent standard deviation of three runs.

Fig. 4. GC-MS chromatographs of (a) raw wastewater and (b) treated by combined microbubble-ozonation/UV process.

Fig. 5. The removal efficiency of COD_{cr} and UV_{254} in microbubble-ozonation/UV combined process and separated processes. Error bars represent standard deviation of three runs.

Fig. 6. The influence of *t*-BuOH concentration on COD_{cr} removal for the combined microbubble-ozonation/UV process; Error bars represent standard deviation of three runs.

Fig. 7. The quantities of hydroxyl radicals produced in ozone water, UV water and the combined ozone/UV water under different conditions as represented with 3D-EEM intensity of the HTA generated.

Fig. 8. The influence of UV irradiation and aeration approaches on ozone decomposition.

Tables caption:

Table1. Characteristics of the acrylic fiber wastewater from all 90 experimental batches.

Table 2. The main organic pollutants identified in the secondary effluent with GC-MS.

Table 3. Variation of COD_{cr}, UV_{254}, and BOD_5/COD_{cr} in microbubble-ozonation alone, UV alone, and the combined microbubble-ozonation/UV process after 120 min reaction.

Table1. Characteristics of the acrylic fiber wastewater from all 90 experimental batches.

Parameter	COD_{cr} (mg/L)	BOD_5 (mg/L)	TOC (mg/L)	NH_3-N (mg/L)	Total Nitrogen (mg/L)	UV_{254} (Abs/cm)	BOD_5/COD_{cr}	pH
Range of values	275-345	40-100	90-145	50-72	75-90	0.35-0.50	0.08-0.21	6.5-8.3
Mean ± S.D.	322 ± 25	59 ± 16	113 ± 19	65 ± 7	82 ± 8	0.42 ± 0.05	0.18 ± 0.02	8.0 ± 0.3

Note: S.D. is the abbreviation of standard deviation.

Table 2. The main organic pollutants identified in the secondary effluent with GC-MS.

No.	Retention Time (min)	Chemicals	Similarity (%)	Area (Mean ± S.D.)	Removal efficiency (%) (Mean ± S.D.)
1	7.492	Toluene	92	91455 ± 1901	99.3 ± 0.5
2	9.783	Ethyl-benzene	90	52645 ± 1102	94.7 ± 0.7
3	10.000	1,2-dimethyl-benzene	88	82014 ± 1637	97.9 ± 1.1
4	10.508	Ethenyl-benzene	90	703290 ± 16134	100 ± 0.0
5	11.142	*N,N*-dimethylacetamide	81	12103 ± 304	100 ± 0.0
6	12.083	Benzenol	93	42964 ± 989	99.0 ± 0.8
7	12.642	Decane	95	43010 ± 710	78.5 ± 1.3
8	13.742	Sulfurous acid, hexyl octyl ester	86	43853 ± 1104	85.9 ± 1.9
9	13.950	2-Methyleneglutaronitrile	92	18243 ± 380	90.8 ± 1.3
10	15.733	2-Phenyl-tridecane	84	112885 ± 2493	94.5 ± 1.6
11	16.367	Pentadecane	96	205338 ± 3390	79.3 ± 1.7
12	16.742	Oxalic acid, 4-chlorophenyl octyl ester	82	31842 ± 855	99.3 ± 1.5
13	16.983	Adipic acid, ethyl methyl ester	85	41622 ± 883	88.4 ± 1.9
14	18.717	Heptadecane	91	189164 ± 4264	84.8 ± 1.3
15	19.567	Hexadecane	91	165455 ± 3067	82.3 ± 2.3
16	20.900	Eicosane	92	65726 ± 1653	88.0 ± 0.9
17	21.242	2,4-Di-*tert*-butylphenol	88	60303 ± 1254	97.8 ± 1.1
18	22.383	Heneicosane	92	71895 ± 1717	88.1 ± 2.4
19	23.333	Pentacosane	92	669806 ± 15393	90.0 ± 2.1
20	23.800	Dotriacontane	93	588049 ± 9993	92.1 ± 1.5
21	25.300	Tetracosane	92	97405 ± 2026	89.0 ± 1.2
22	26.925	Hexatriacontane	93	161151 ± 4117	93.8 ± 1.4
23	27.117	Tetracontane	91	578067 ± 12530	95.6 ± 1.1

Table 3. Variation of COD_{cr}, UV_{254}, and BOD_5/COD_{cr} in microbubble-ozonation alone, UV alone, and the combined microbubble-ozonation/UV process after 120 min reaction.

Items	COD_{cr} removal (%)	UV_{254} removal (%)	Improvement of BOD_5/COD_{cr}
Microbubble-ozonation alone	23.2	50.5	0.09
UV irradiation alone	5.0	14.1	0.03
Microbubble-ozonation/UV combined process	92.5	83.4	0.29
Synergistic efficiency (%)	228	29	142

Note: the improvement of BOD_5/COD_{cr} was the D-value between the BOD_5/COD_{cr} at 120 min and the initial BOD_5/COD_{cr}.

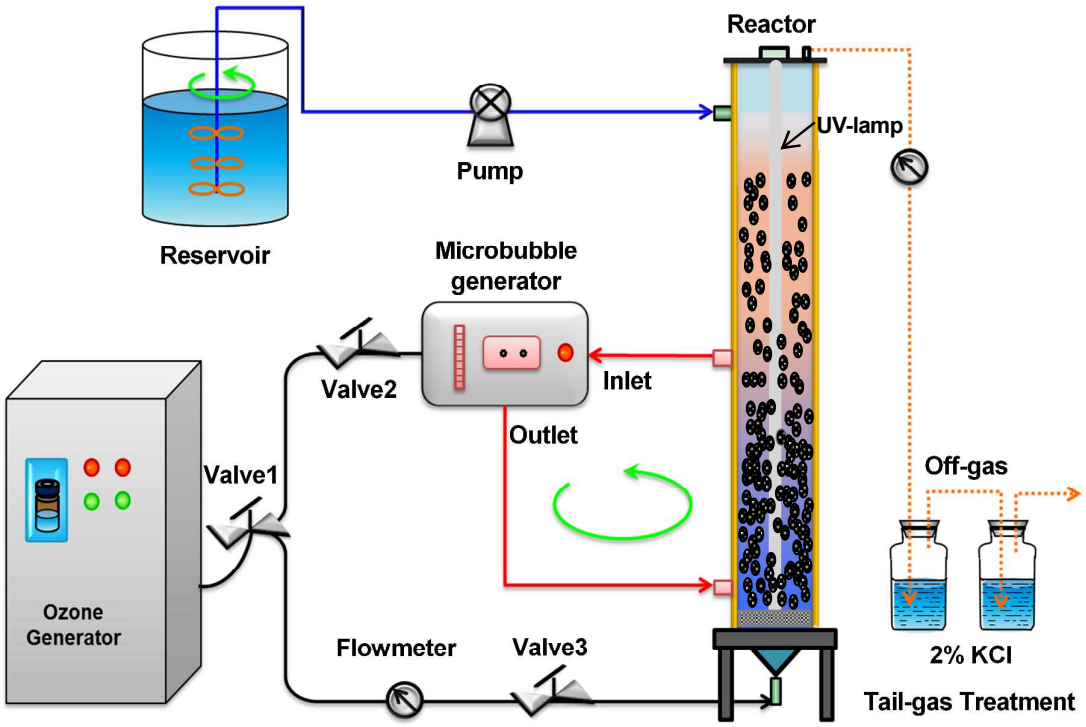

Fig. 1. Schematic diagram of microbubble-ozonation/UV combined process experimental setup.

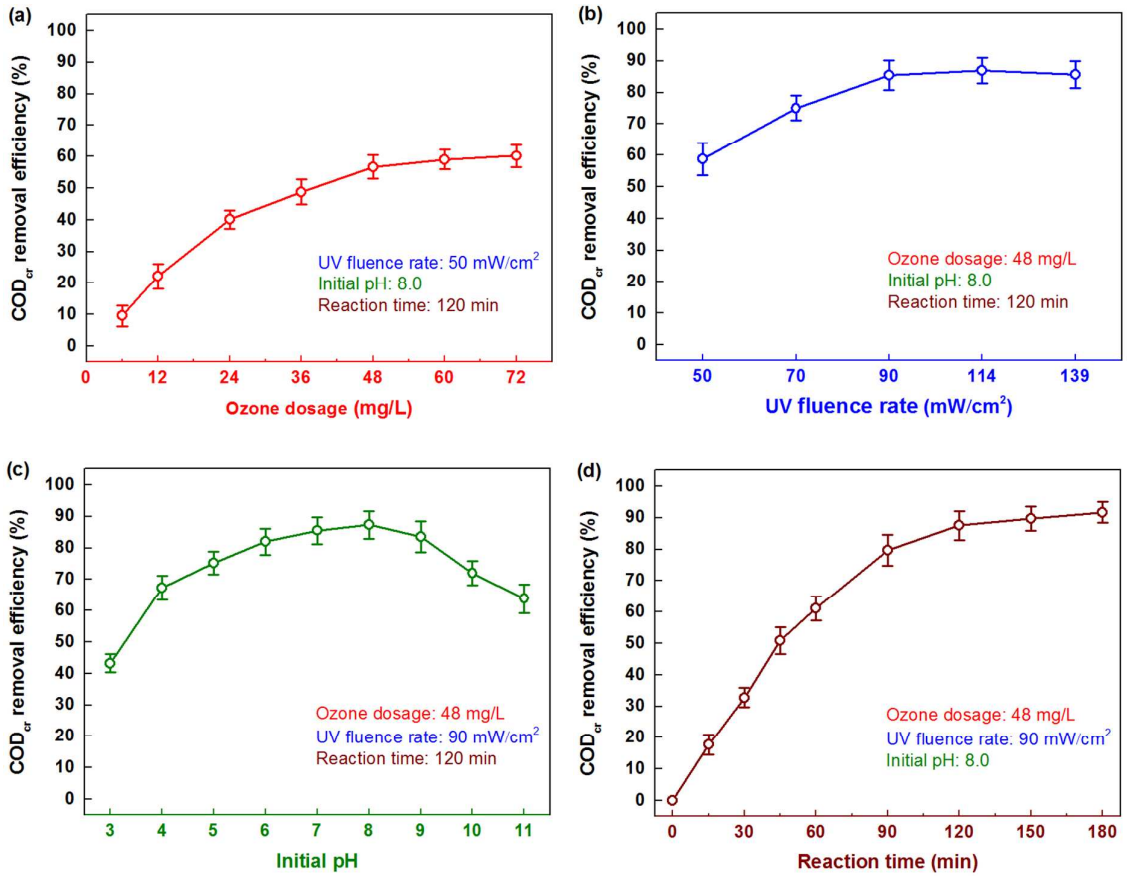

Fig. 2. Influences of different parameters on the COD_{cr} removal efficiency in the microbubble-ozonation/UV combined system. (a) ozone dosage, (b) UV fluence rate, (c) initial pH and (d) reaction time. Error bars represent standard deviation of three runs.

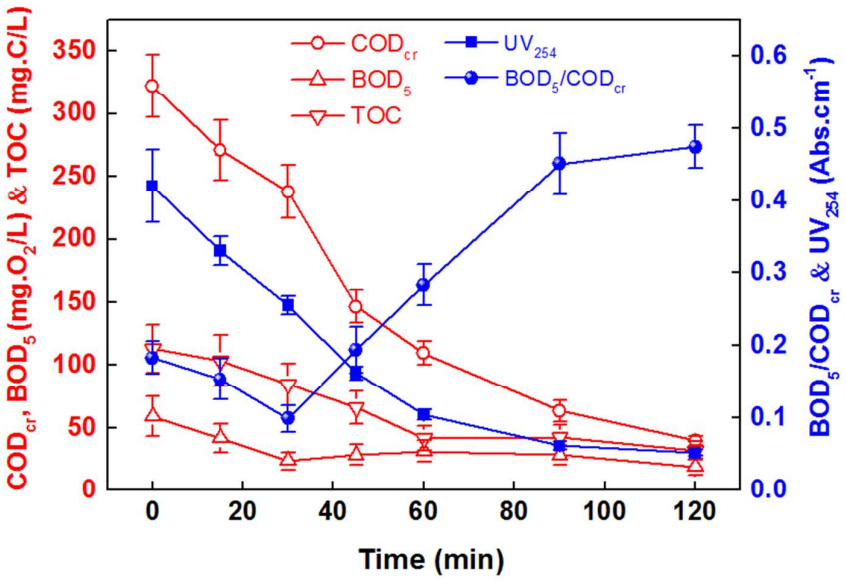

Fig. 3. Degradation of contaminants over time in the microbubble-ozonation/UV reactor under optimized conditions (i.e., ozone dosage of 48 mg/L, UV fluence rate of 90 mW/cm^2, initial pH value of 8.0 and reaction time of 120 min). Error bars represent standard deviation of three runs.

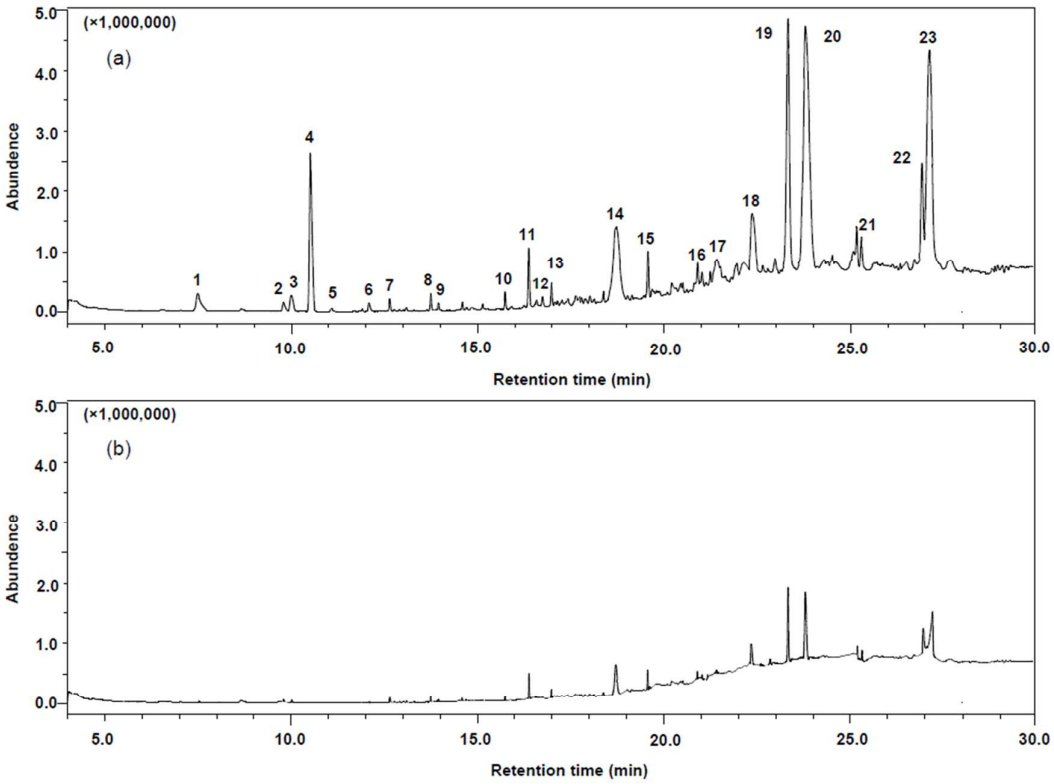

Fig. 4. GC-MS chromatographs of (a) raw wastewater and (b) treated by combined microbubble-ozonation/UV process.

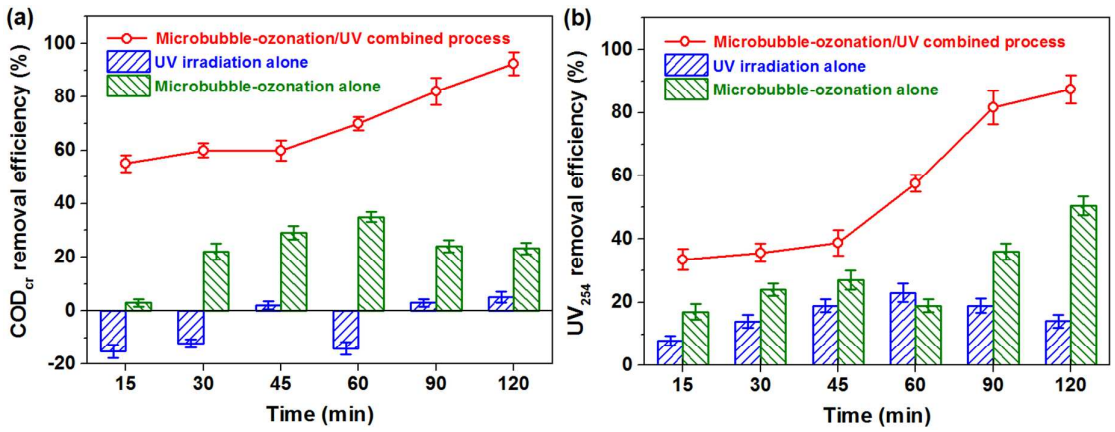

Fig. 5. The removal efficiency of COD_{cr} and UV_{254} in microbubble-ozonation/UV combined process and separated processes.

Error bars represent standard deviation of three runs.

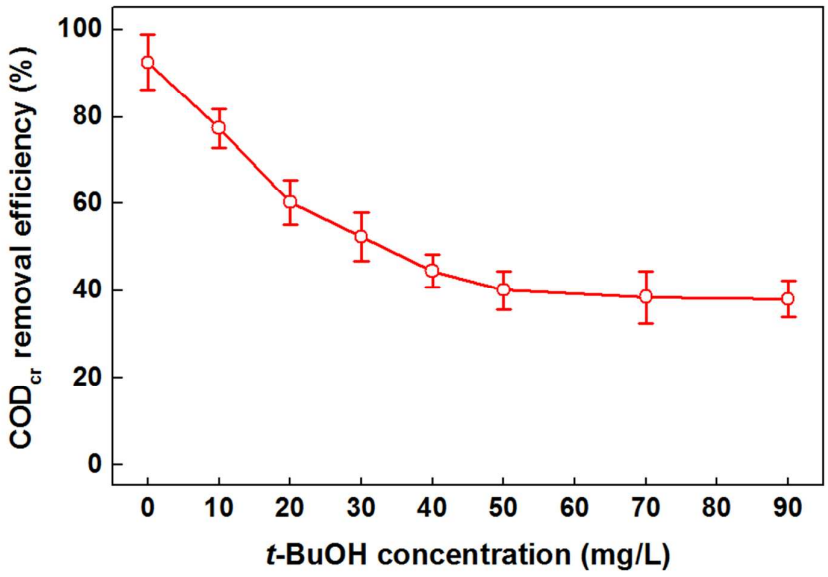

Fig. 6. The influence of *t*-BuOH concentration on COD_{cr} removal for the combined microbubble-ozonation/UV process; Error bars represent standard deviation of three runs.

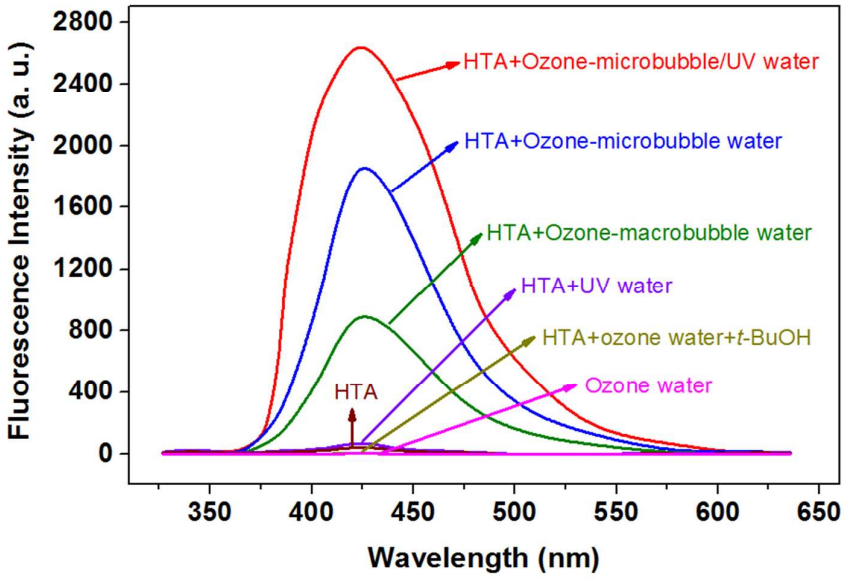

Fig. 7. The quantities of hydroxyl radicals produced in ozone water, UV water and the combined ozone/UV water under different conditions as represented with 3D-EEM intensity of the HTA generated.

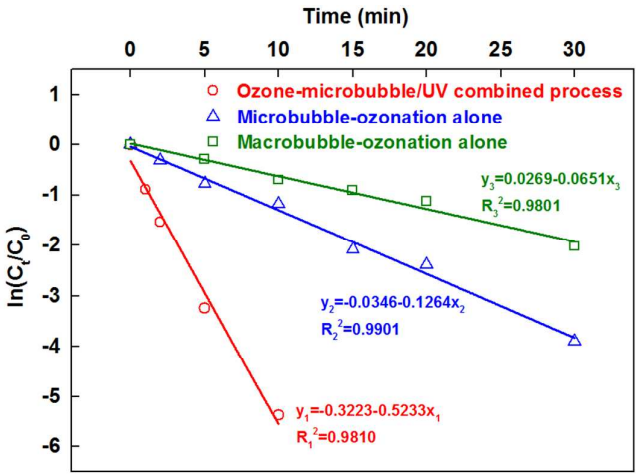

Fig. 8. The influence of UV irradiation and aeration approaches on ozone decomposition.